Journal of
Microscopy

Journal of Microscopy, Vol. 00, Issue 0 2016, pp. 1–7
Received 22 October 2015; accepted 2 May 2016

doi: 10.1111/jmi.12428

Titanium diffusion in shinbone of rats with osseointegrated implants

MIRIAM S. GRENÓN*, JOSÉ ROBLEDO†,§, JUAN CARLOS IBÁÑEZ‡ & HÉCTOR J. SÁNCHEZ†,§
**Facultad de Odontología, Universidad Nacional de Córdoba, Córdoba, Argentina*
†Facultad de Matemática, Astronomía y Física, Universidad Nacional de Córdoba, Córdoba, Argentina
‡Facultad de Medicina, Universidad Católica de Córdoba, Córdoba, Argentina
§CONICET, Argentina

Key words. Dental implants, microXRF, newly formed bone diffusivity, synchrotron radiation.

Summary

Dental implants are composed of commercially pure Ti (which is actually an alloy of titanium, and minor or trace components such as aluminium and vanadium). When the implant is inserted, its surface undergoes a number of chemical and mechanical processes, releasing particles of titanium to the medium. The metabolism of free ions of titanium is uncertain; the uptaking processes in the body are not well known, nor their toxic dose. In addition, physical properties of newly formed bone, such as diffusivity and activation energy, are scarce and rarely studied. In this study, we analysed the diffusion of titanium in the titanium-implanted shinbones of six adult male Wistar rats by spatially resolved micro x-ray fluorescence. The measurements were carried out at the microfluorescence station of the x-ray fluorescence (XRF) beamline of the Brazilian synchrotron facility LNLS (from Portuguese '*Laboratorio Nacional de Luz Sincrotron*'). For each sample, XRF spectra were taken by linear scanning in area near the new bone formed around the Ti implant. The scanning line shows a clear effect of titanium diffusion whereas calcium intensity presents a different behaviour. Moreover, a clear correlation among the different structures of bones is observed in the Ti and Ca intensities. The results obtained in these measurements may allow determining quantitatively the parameters of diffusion rates and other physical properties of new bone like diffusion coefficients.

Introduction

Titanium is a transition element extremely resistant to corrosion; it is present at trace levels in tissues and body fluids. Nevertheless, these Ti concentrations are not well established. There are reported studies of the behaviour of titanium concentrations in supra- and infragingival dental calculus, with different stages of maturation (Sánchez *et al.*, 2000; Abraham *et al.*, 2002; Pérez *et al.*, 2004; Abraham *et al.*, 2005; Sánchez *et al.*, 2008; Abraham *et al.*, 2010). These studies also analyse the saliva and gingival fluid, corresponding to healthy and ill subjects, smokers and nonsmokers, postmenopausal women with osteopenia and osteoporosis, patients affected by periodontal disease with and without treatment, and people with different calcium intake in their diet. These results show large variations in the concentration of titanium (Sánchez *et al.*, 2008; Abraham *et al.*, 2010). Another survey analysed the saliva and the gingival fluid of patients with dental implants by total x-ray fluorescence (TXRF) with synchrotron radiation (SR; Abraham *et al.*, 2014). The mean concentration of Ti measured in saliva was (3.5 ± 0.5) ppm in patients without implants and (2.8 ± 0.5) ppm in patients with implants. Nevertheless, the concentration of Ti in gingival fluid was (1.3 ± 0.4) ppm in patients without implants and (22 ± 7) ppm for those with implants. This shows that patients with implants seem to have greater concentrations of Ti in their gingival fluid than those without implants, whereas the concentration of Ti in their saliva seems to be unaffected by the implant.

These results, together with the scarce knowledge about the effect of titanium in humans, provide a better understanding of the diffusion processes of titanium ions coming from implants in bones (Tawse-Smith *et al.*, 2012). In addition, the study of diffusion processes will provide relevant information about the physical properties of newly formed bone around the implants. There are some parameters, which are barely known, that are a long overdue of human knowledge, such as diffusivity (diffusion coefficient), activation energy, among others.

The micro-X ray fluorescence technique (μXRF) is a suitable method for measuring trace elements in small samples with spatial resolution (Van Grieken & Markowicz, 2002). This

Correspondence to: Héctor J. Sánchez, Facultad de Matemática, Astronomía y Física, Universidad Nacional de Córdoba, Córdoba, Argentina. Tel/Fax: +54 351 4334051; e-mail: jsan@famaf.unc.edu.ar

spectrochemical technique is nondestructive and provides the quantification of major, minor and trace elements with a very good sensitivity and detection limits for transition elements. The quantification results obtained with this technique can be improved if combined with SR. The x-rays that are produced in a synchrotron have outstanding properties: high degree of natural collimation, high degree of polarization, pulsed time structure, high intensity, very broad and continuous spectral range from infrared up to the hard x-ray region, and high brilliance of the source, among others (Koch, 1983). The natural collimation of SR, in combination with an adequate focusing optics represents a significant advantage in order to obtain reliable spatially resolved data. Besides, the high intensity of SR allows the use of monochromators, which provide a tunable source of photons, giving the possibility of selective irradiation.

In this work, spatially resolved x-ray fluorescence analysis, induced by SR, was used to analyse the diffusion of Ti-ions through the newly formed bone of shinbones of rats. We measured the spatial pattern of diffusion and, with this data, we obtained information about the properties of newly formed bones.

Experimental

Six adult male Wistar rats, weighing 180 ± 60 g, were studied. General anesthesia was administered with 2% xylazine/ketamine 5%. The shinbone of each animal was prepared for surgery by presurgical shaving and sterilizing the skin. A vertical incision of 1.5 cm was performed, and a hole in the cortex was carried out with a sterile round bur by manual pressure. A single pure (>99.999%) titanium foil of 1.5 mm × 0.3 mm and 4-mm thick was introduced in the perforation, inside the bone, in the longitudinal direction. Finally, nylon suture 4-0 was used for suturing. Figure 1 shows an osseointegration control by x-ray radiography (RX) of one of the samples after the surgery.

A month after the titanium insertion, Euthanasia was done to a first group of three random rats, and 2 months later to the remaining three rats (a total of 3 months since the titanium insertion). Dried tibiae were preserved in 10% formalin. Soft tissue was removed with a plastic surgical clamp, RX's were taken, and bones were included in a self-curing acrylic for subsequent cross-section cuts. All the elements and tools used in the preparation of the samples were checked to be free of titanium in order to avoid contaminations. The self-curing acrylic was liquid monomer Vaicel, manufactured by Vaicril Labs. S.A. (Argentina) and the plastic surgical clamps were Aviodent N°5 manufactured by Odontopack S.A. (Argentina). Animals care and surgery were performed under International Animal Protection Rules (National Institutes of Health). The subsequent measurements were performed no more than 3 days after tibiae dissection. It was verified that during the healing, no wound became infected and all the titanium sheets were osseointegrated.

Fig. 1. RX control of implant osseointegration (arrows) of a typical sample.

The experiments were carried out in the high-vacuum station of the XRF beamline at the Synchrotron Light National Laboratory (LNLS, Campinas, Brazil) (Pérez *et al.*, 1999). The electron energy inside the storage ring is 1.37 GeV with a dipole magnetic field of 1.67 T, which produces a critical photon energy of 2.08 keV. The SR source for the XRF beamline is the D09B bending magnet (15°) of the storage ring. The components of the beamline include a 125-μm-thick beryllium window to isolate the beamline vacuum from the ring vacuum and from the atmosphere, a Si(111) double crystal channel-cut monochromator of ∼3 eV resolution at 10 keV, and a motorized computer-controlled set of slits to limit the beam size. The photon flux on the sample was of $\sim 10^8 \frac{ph}{2}$. A Si(Li) energy-dispersive detector was used in the measurements of this work, which was placed at 90° with respect to the incident beam in order to minimize Compton and Rayleigh scattering contribution to the spectra. The pulse processing was accomplished by a fast amplifier with triangular shaping and spectra were collected with a 8K MCA.

All of the measurements were performed in conventional (45° + 45°) geometry, using a monochromatic beam of 5100 eV to excite the Ti-K edge. The experiments were performed in an air atmosphere. A fine conical monocapillary focused the white beam into a small area, producing the desired microbeam. A polycapillary was set between the sample and

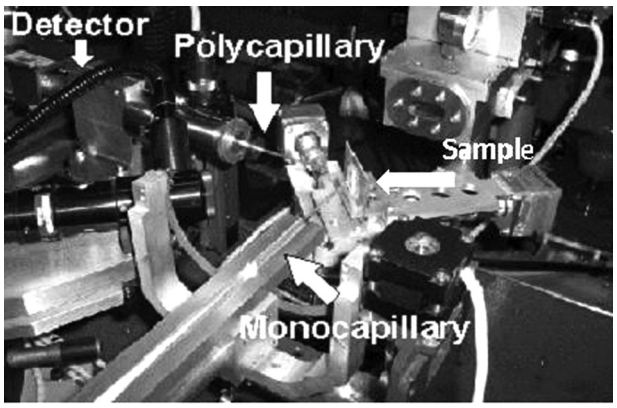

Fig. 2. The experimental setup of the XRF endstation at the LNLS.

the detector as to select the photons that come from the desired microarea, and as to increase the photon flux coming from this region to the detector, that is, as to decrease the measuring times. All measurements were performed selecting the sampled area with an optical microscope, which is placed perpendicular to the sample surface. The actual beam size on the sample was $10 \times 10\ \mu m^2$ and the positioning resolution (step size) was $1\ \mu m$. For each sample, XRF spectra were taken by linear scanning in the area near the newly formed bone around the Ti implant. This procedure was performed using a XYZ positioning stage having a 1-μm accuracy. Figure 2 shows the experimental setup of the XRF endstation and a schematic of the setup for better understanding. Figure 3 shows a microphotograph of the implant, the newly formed bone around, and the line of irradiation under analysis. Depending on the sample, between 15 and 30 points were measured during the linear scanning. The measuring time per point varied from 500 to 700 s.

Data analysis and results

All of the spectra were analysed using a conventional program for spectrum analysis (Solé *et al.*, 2007) as to obtain the net intensity of the elements present in the samples. With this program, a background model of a 9° orthogonal polynomial, escape peaks, and peak-shape corrections were applied. Figures 4 and 5 show the measured intensities of Ca and Ti corresponding to the sample shown in Figure 3 normalized by the storage ring current (incident intensity).

Diffusion theory

Diffusion of free ions in a solid-state structure can be explained by means of the Fick´s Laws (Crank, 1973). The 1st Fick´s Law states that, at steady state, the diffusive flux goes from regions of high concentration to regions of low concentration, and it is proportional to the concentration gradient:

$$J = -D\vec{\nabla}c, \tag{1}$$

where J is the diffusive flux of ions, c is the concentration of ions as a function of the position and D is the diffusion coefficient or diffusivity. The units of J are given in ions per unit area per unit time (i.e. mass/lenght^2 $\times$ time), the diffusivity D has units of unit area per unit time (i.e. lenght^2/time). For steady state, the continuity equation indicates

$$\frac{\partial c}{\partial t} = -\vec{\nabla}J \tag{2}$$

and combining (1) and (2), we obtain the 2nd Fick´s law (diffusion equation)

$$\frac{\partial c}{\partial t} - D\nabla^2 c = 0.$$

Assuming that the diffusive flux is in one dimension:

$$\left(\frac{\partial c}{\partial t}\right)_x = D\left(\frac{\partial^2 c}{\partial x^2}\right)_t$$

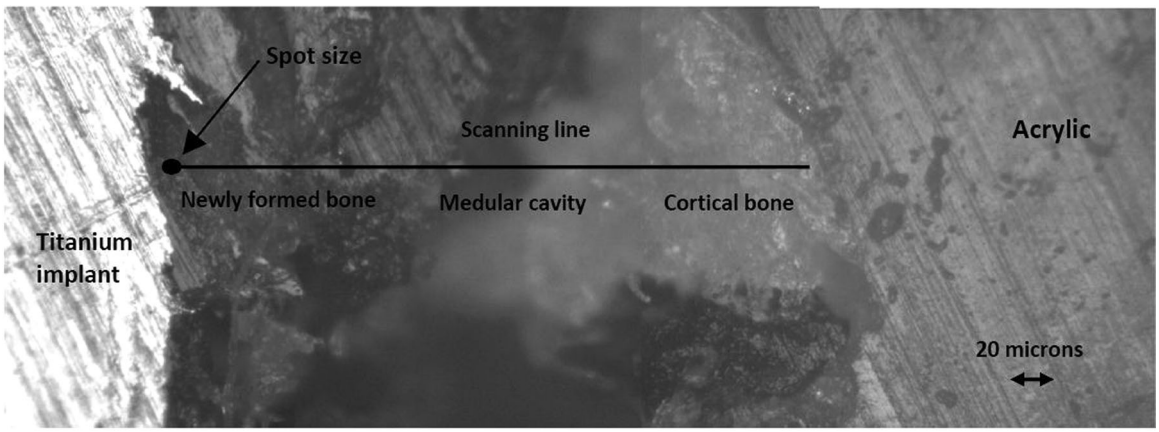

Fig. 3. Microphotograph of an implant in a typical sample, the newly formed bone around, and the line of irradiation under analysis. This sample corresponds to a shinbone after 3 months implantation.

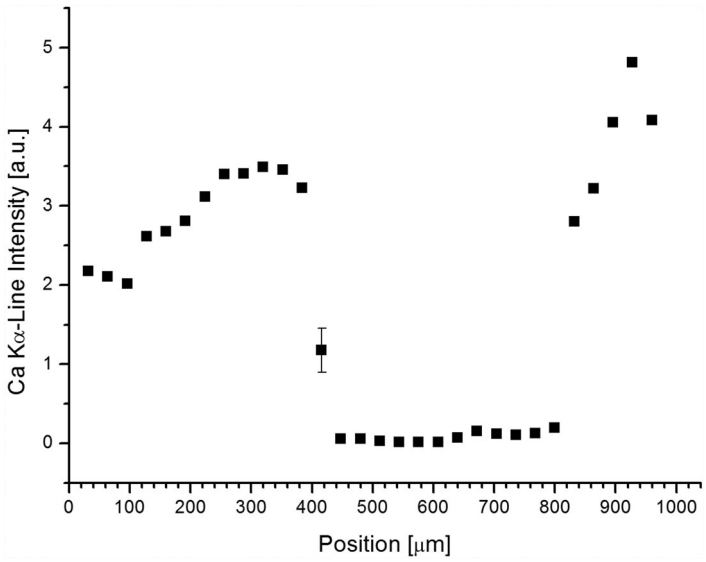

Fig. 4. Measured intensities of Ca corresponding to the sample shown in Figure 3 (a shinbone after 3 months implantation) normalized by the storage ring current (incident intensity).

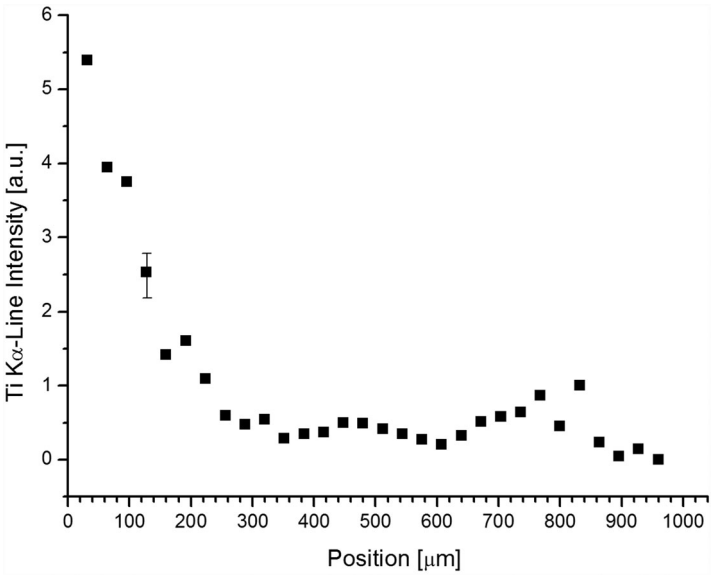

Fig. 5. Measured intensities of Ca corresponding to the sample shown in Figure 3 (a shinbone after 3 months implantation) normalized by the storage ring current (incident intensity).

which postulates that the variation of the concentration with time is proportional to the curvature of the concentration profile.

The solution of the diffusion equation is

$$c\,(x,t) = c\,(0,t)\left[1 - erf\left(\frac{x}{2\sqrt{Dt}}\right)\right],$$

where *erf* stands for the error function, and is given by

$$erf\,(x) = \frac{2}{\pi}\int_0^x e^{-t^2}dt.$$

By means of the solution of the diffusion equation, the diffusivity D can be obtained from

$$erf^{-1}\left[1 - \frac{c\,(x,t)}{c\,(0,t)}\right] = \left(\frac{1}{2\sqrt{Dt}}\right)x, \qquad (3)$$

where $erf^{-1}(x) = \sum_{k=0}^{\infty}\frac{c_k}{2k+1}(\frac{\sqrt{\pi}}{2}x)^{2k+1}$, by performing a linear fitting of $erf^{-1}[1 - \frac{c(x,t)}{c(0,t)}]$ versus x.

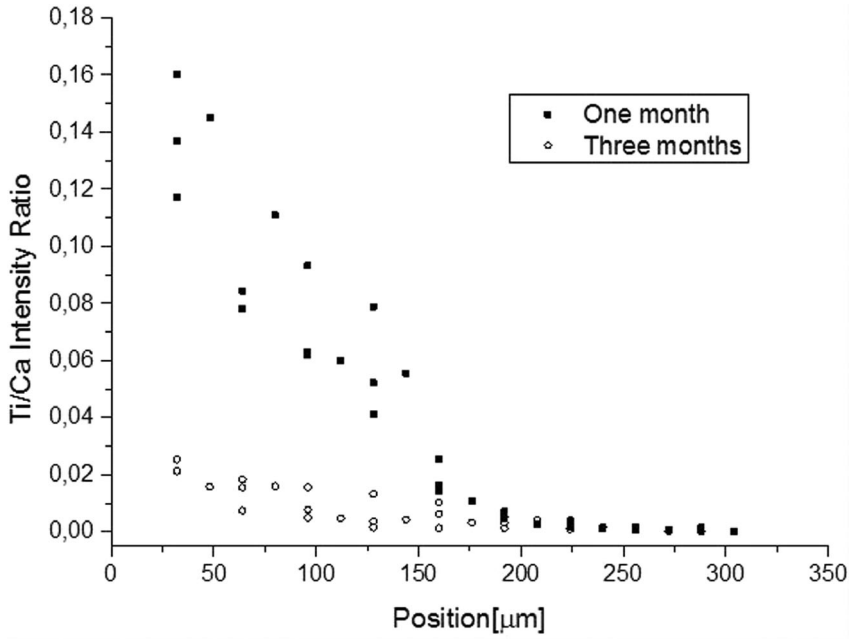

Fig. 6. Normalized intensity of titanium as a function of the position.

Normalization

The measured intensity of the peak that corresponds to a specific element is not a direct measurement of its concentration due to matrix effects, enhancements and sample's density. Although matrix effects and enhancements are the same for all the measurements in a given sample, density can present different values at different position in the sample during the spatial scanning. In samples based on octocalcium phosphates, as the ones analysed in this paper, calcium is a major element and its intensity (counts) is approximately proportional to the concentration (Brown & Constantz, 1994); in addition, the concentration has a linear correlation with the density and with the degree of compaction of the crystal structure. Using these properties of octocalcium phosphates a representative value of the concentration of Ti can be obtained by calculating the intensity ratio Ti/Ca in each position, so the calcium intensity acts like a normalization factor for each measurement. This ratio is an absolute value, independent of the local density and proportional to the variation of the concentration of titanium as a function of the position within the newly formed bone around the implanted material. Figure 6 shows the normalized intensity (in arbitrary units) of titanium as a function of the position.

Fitting

The Ca-normalized titanium intensities, for every position in all samples, were collected and grouped in two sets, corresponding to the time of osseintegration (1 month and 3 months). Then, a linear fit according to Eq. (3) was performed. Figure 7 shows the measured titanium data transformed according to the erf^{-1} function versus the distance to the implant (x) for the two sets of data, and the corresponding linear fit. The fitted parameters are shown in Table 1.

Table 1. Slope, Intercept and Diffusivity at two different times after implantation

	Slope $\left[\frac{1}{\mu m}\right]$	Intercept (y)	$D\left[\frac{\mu m^2}{day}\right]$
One month	0.0061 ± 0.0003	0.04 ± 0.05	224 ± 23
Three months	0.0076 ± 0.0003	-0.04 ± 0.06	48 ± 3

The y-intercept of both linear regressions includes the zero value, as expected. From the slopes (denoted a), the diffusion coefficient can be calculated as $D = \frac{1}{4a^2 t}$. These coefficients are shown in the third column of the table.

Discussion

As can be seen in Figures 4 and 5, there is a clear effect of titanium diffusion whereas calcium is concentrated at the borders of the shinbone. Moreover, a clear correlation among the different structures of bones is observed in the Ti and Ca intensities. Nevertheless, the titanium diffusion seems to be small compared to the diameter of the shinbone.

Figure 6 shows the patterns of diffusion of ions for the titanium concentrations, indicating the effective use of the Ca intensity as a normalizing factor. It can be observed from this figure that titanium diffuses mainly on the newly formed bone around the implant (radially around 150 μm from the

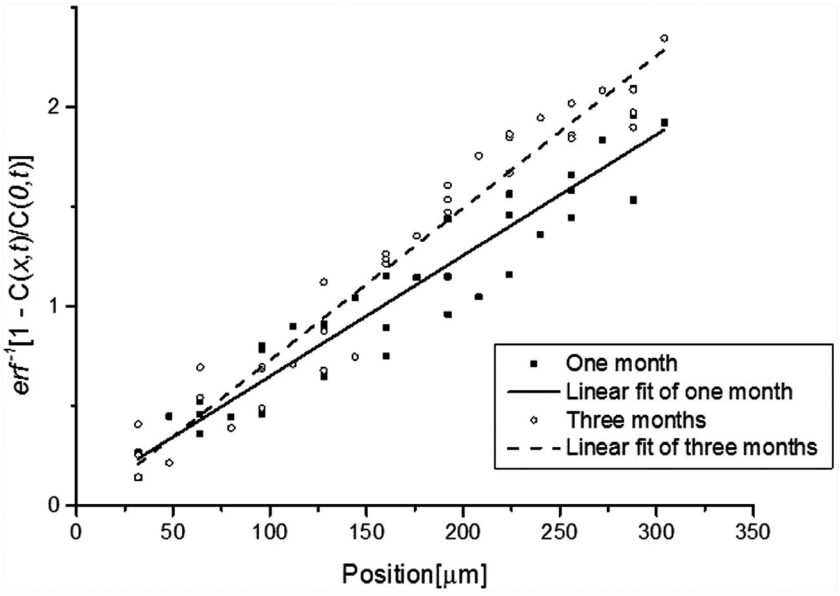

Fig. 7. Measured titanium data transformed according to the erf-1 function versus the distance to the implant (x) for the two sets of data, and the corresponding linear fit.

implant). All the samples presented more or less a similar pattern of diffusion. The sudden drops of intensity, which can be observed in the figures, correspond to holes in the newly formed bone or in the medullar cavity.

As far as the authors knowledge, Table 1 shows for the first time the diffusivity of newly formed bone. In this context, the absolute value of diffusivity has a relative significance; however, the comparison of diffusion coefficients for different stages of bone growth indicates a clear variation of diffusion permeability as the bone grows. A higher value of diffusivity for younger bone (1 month) means that titanium ions migrate out from the implant with a greater flux. On the other side, 'older' formed bone present a lower diffusion coefficient, which indicates a more compact structure, possibly a brushite turning into a whitlockite or even apatite, making more difficult the migrations of ions.

Conclusions

In this work, the diffusion coefficients for titanium diffusion in the shinbones of Wistar rats were successfully obtained by studying the intensity ratio Ti/Ca in spectra measured by micro x-ray fluorescence induced by SR. A similar diffusion is observed in rats having the implant for a month than in rats having the implant for 3 months. As expected, the diffusion coefficient is larger for the group of rats that had the implant for a shorter time.

The limitations of this study are typical of this kind of work. Even considering typical rats, using ultra-pure materials, standardized surgical procedures and state-of-the-art spectroscopy techniques, biological systems has a significant variability. Measured diffusivities are indeed approximate values. However, they have two important qualities: they represents the first values ever reported and they show the behaviour of the diffusion coefficient with the time.

Further investigations are needed to obtain a greater set of diffusion coefficients' data. This will allow a better understanding of the processes of bone formation around implants and, eventually, will permit quantifying the total amount of titanium delivered to the body by the presence of the implant.

Acknowledgement

This work has been partially supported by the Brazilian Synchrotron Light Laboratory (LNLS).

References

Abraham, J., Grenón, M., Sánchez, H.J., Pérez, C. & Barrea, R. (2002) Spectrochemical analysis of dental calculus by synchrotron radiation X-ray fluorescence. *Anal. Chem.* **74**, 324–329.

Abraham, J., Grenón, M., Sánchez, H.J., Pérez, C. & Barrea, R. (2005) A case study of elemental and structural composition of dental calculus during several stages of maturation using SRXRF. *J. Biomed. Mater. Res.* **75A**, 623–628.

Abraham, J., Sánchez, H.J., Grenón, M.S. & Pérez, C.A. (2014) TXRF analysis of metals in oral fluids of patients with dental implants. *X Ray Spectrometr.* **43**, 193–197.

Abraham, J., Sánchez, H.J., Grenón, M.S. & Valentinuzzi, M.C. (2010) Influence of smoking in the elemental composition of oral fluids. *X Ray Spectrometr.* **39**, 372–375.

Brown, P.W. & Constantz, B. (1994) *Hydroxyapatite and Related Materials*. CRC Press Inc., Boca Raton, USA.

Crank, J. (1973) *The Mathematics of Diffusion*. 2nd edn. Oxford Science Publications, USA.

Koch, E. (1983) *Handbook of Synchrotron Radiation*. North-Holland, Amsterdam.

National Institutes of Health. Office of laboratory animal welfare – Public Health Service Policy on Humane Care and Use of Laboratory Animals. Available at: http://grants.nih.gov/grants/olaw/references/phspol.htm (2015)

Pérez, C., Radke, M., Sánchez, H.J. *et al*. (1999) Synchrotron radiation X-ray fluorescence at the LNLS: beamline instrumentation and experiments. *X Ray Spectrometr.* **28**, 320–326.

Pérez, C., Sánchez, H.J., Grenón, M., Abraham, J. & Barrea, R. (2004) Microscopic X-ray fluorescence analysis of human dental calculus using synchrotron radiation. *J. Anal. Atomic Spectrometr.* **19**, 392–397.

Sánchez, H.J., Pérez, C.A. & Grenón, M. (2000) SRXRF analysis with spatial resolution of dental calculus. *Nucl. Instr. Meth.* **B170**, 211–218.

Sánchez, H.J., Valentinuzzi, M.C., Grenón, M. & Abraham, J. (2008) Total reflection X-ray fluorescence analysis of oral fluids of women affected by osteoporosis and osteopenia. *Spectrochemical Acta B* **63**, 1485–1488.

Solé, V.A., Papillon, E., Cotte, M., Walter, P. & Susini, J. (2007) A multiplatform code for the analysis of energy-dispersive X-ray fluorescence spectra. *Spectrochimica Acta B* **62**, 63–68.

Tawse-Smith, A., Ma, S., Siddiqi, A., Duncan, W.J., Girvan, L. & Hussaini, H.M. (2012) Titanium particles in peri-implant tissues: surface analysis and histologic response. *Clin. Adv. Peridont.* **2**, 232–238.

Van Grieken, R. & Markowicz, A. (2002) *Handbook of X-Ray Spectrometry*. 2nd edn. Marcel Dekker, New York.